Available online at http://scik.org
J. Math. Comput. Sci. 6 (2016), No. 5, 875-893
ISSN: 1927-5307

STUDY ON THE DIFFERENTIAL PROPERTIES OF A ROBOT END-EFFECTOR MOTION USING THE CURVATURE THEORY

RAWYA A. HUSSIEN* AND ALI ABDELA ALI

Mathematics Department, Faculty of Science, Assiut University Assiut 71516, Egypt

Abstract. In this paper, tool trihedron for timelike ruled surface with spacelike ruling and spacelike directrix is constructed. Transition relations among surface trihedron, tool trihedron, generator trihedron, natural trihedron and also Darboux vectors for each trihedron are obtained. Then, the curvature theory of the constructed frame is applied to determine the differential properties of the motion. Finally the dynamical motion of the tool frame along the trajectory planning is determined.

Keywords: Timelike ruled surface; Darboux vector; Robot trajectory planning; Robot end-effector.

2010 AMS Subject Classification: $53A05$, $53A17$, $53B30$.

1. Introduction

The methods of robot trajectory control are currently used and are based on PTP (point to point) and CP (continuous path) methods. These methods are basically interpolation techniques and, therefore, are approximations of the real path trajectory . In such cases, when a precise trajectory is needed, or we need to trace a free formed or analytical surface accurately, the precision is only proportional to the number of intermediate data points for offline programming. For accurate robot trajectory, the most important aspect is the continuous representation

*Corresponding author

Received March 3, 2016

of orientation where as the position representation is relatively easy. There are methods such as homogeneous transformation, Quaternion, and Euler Angle representation to describe the orientation of a body in a three dimensional space . These methods are easy in concept but have high redundancy in parameters and are discrete representation in nature rather than continuous. Therefore, a method based on the curvature theory of a ruled surface has been proposed as an alternative . Ruled surfaces are widely used in many areas in modern surface modelling systems. The ruled surfaces are surfaces swept out by a straight line moving along a curve and the study of ruled surfaces is an interesting research area in the theory of surfaces in Euclidean geometry. Theory of ruled surfaces is developed by both surface theory and E. Study map which enables one to investigate the geometry of ruled surfaces by means of one real parameter. It is also known that theory of ruled surfaces is applicable to theoretical kinematics.

1.1. Minkowski space [1,6]

Let R^3 be a real 3-dimensional vector space with a metric tensor

$$\prec,\succ: R^3 \times R^3 \to R, \qquad \prec \underline{V},\underline{W} \succ = V_1W_1 + V_2W_2 - V_3W_3$$

such that $\prec \underline{V},\underline{W} \succ$ is a non degenerate symmetric bilinear form, the pair $(R^3,\prec,\succ)$ is called Minkowski (Lorentz) space and is denoted by ${R_1}^3$.

Definition 1.1 A vector $\underline{V}$ in lorentz space ${R_1}^3$ is called

(i) Spacelike if $\prec \underline{V},\underline{V} \succ > 0, or \underline{V} = 0$

(ii) Timelike if $\prec \underline{V},\underline{V} \succ < 0$

(iii) Lightlike (Null)if $\prec \underline{V},\underline{V} \succ = 0, for \underline{V} \neq 0$.

Definition 1.2 Let ξ be the set of all timelike vectors in Lorentz vector space V. For $\underline{v} \in \xi$, the set

$$C(\underline{v}) = \{\underline{w} \in \xi : \prec \underline{v},\underline{w} \succ < 0\}$$

is the lightcone V of containing

Lemma 1.1 Timelike vectors $\underline{V}$ and $\underline{W}$ in Lorentz space are in the same timecone if and if only $\prec \underline{V},\underline{W} \succ < 0$.

Definition 1.3 The vectors $\underline{V}$ and $\underline{W}$ in Lorentz space are called orthogonal if and only if

$\prec \underline{V}, \underline{W} \succ = 0$.

Lemma 1.2 If $\underline{V}$ and $\underline{W}$ are in the same timecone of ${R_1}^3$ there is a unique number $\phi \geq 0$ is called the hyperbolic angle between $\underline{V}$ and $\underline{W}$ such that

$$\prec \underline{V}, \underline{W} \succ = -\|\underline{V}\| \|\underline{W}\| \cosh \phi.$$

Lemma 1.3 If $\underline{V}$ and $\underline{W}$ are timelike and spacelike vectors respectively, then

$$\prec \underline{V}, \underline{W} \succ = -i\|\underline{V}\| \|\underline{W}\| \cosh \phi, where \quad i = \sqrt{-1}.$$

Definition 1.4 let $\underline{V}$ be a vector in Lorentz space ${R_1}^3$. The norm $\|\|$ of a vector $\underline{V}$ is defined as

$$\|\underline{V}\| = \sqrt{| \prec \underline{V}, \underline{V} \succ |}.$$

For any vector $\underline{V}$ in Lorentz space ${R_1}^3$ we have

(i) $\|\underline{V}\| \geq 0$.

(ii) $\|\underline{V}\| = 0 \Leftrightarrow \underline{V}$ be a null vector or $\underline{V} = 0$.

(iii) $\|\underline{V}\|^2 = \prec \underline{V}, \underline{V} \succ \Leftrightarrow \underline{V}$ be spacelike vector.

(iv) $\|\underline{V}\|^2 = - \prec \underline{V}, \underline{V} \succ \Leftrightarrow \underline{V}$ be timelike vector.

Definition 1.5 let $\underline{V}$ and $\underline{W}$ be two vectors in lorentz space. The vectorial product of $\underline{V}$ and $\underline{W}$ is defined as

$$\underline{V} \wedge \underline{W} = \begin{vmatrix} \underline{e}_1 & \underline{e}_2 & -\underline{e}_3 \\ V_1 & V_2 & V_3 \\ W_1 & W_2 & W_3 \end{vmatrix}.$$

A timelike curve $\alpha = \alpha(s) \in {R_1}^3$, parameterized by the natural parametrization, is a frame field $\{e_1, e_2, e_3\}$, having the following properties

(1) $\prec e_1, e_1 \succ = \prec e_2, e_2 \succ = 1, \prec e_3, e_3 \succ = -1$

(2) $e_1 \wedge e_2 = -e_3$,$e_1 \wedge e_3 = -e_2$, $e_2 \wedge e_3 = e_1$

Lemma 1.4 Let $\underline{V}$ and $\underline{W}$ be two vectors in ${R_1}^3$, we have

$\underline{V}$	$\underline{W}$	$\underline{V} \wedge \underline{W}$
$spacelike$	$spacelike$	$timelike$
$spacelike$	$timelike$	$spacelike$
$timelike$	$timelike$	$spacelike$
$timelike$	$null$	$spacelike$
$null$	$null$	$spacelike$
$spacelike$	$null$	$null\ \ if \prec \underline{V}, \underline{W} \succ = 0$
$spacelike$	$null$	$spacelike\ \ if \prec \underline{V}, \underline{W} \succ \neq 0$

1.2.Curves and ruled surfaces in Lorentz space [1]

Definition 1.6 A curve in ${R_1}^3$ is a smooth mapping $\alpha : I \to {R_1}^3$, where I is an open interval in the real line. The velocity vector of α at $s \in I$ is $\underline{\alpha}'(s) = \frac{d}{ds}\underline{\alpha}(s)$. A curve $\alpha = \underline{\alpha}(s)$ is regular provided $\underline{\alpha}'(s) \neq 0$, for all $s \in I$. A curve α in ${R_1}^3$ is said to be a spacelike, timelike and null curve if the velocity vector $\underline{\alpha}'(s)$ is a spacelike, timelike and null (lightlike), respectively

Definition 1.7 A surface M in the Lorentz space is called of type spacelike or timelike according to the induced metric g on M is positive definite or a negative definite (Lorentz) metric, respectively.

Definition 1.8 The surface M is said to be a type spacelike or timelike according to the normal vector $\underline{N}$ on the surface is a timelike vector or a spacelike vector, respectively.

1.3. Robot trajectory planning [2,3,4]

The motion of robot end-effector is referred to as the robot trajectory. A robot trajectory consists of

(i) A sequence of positions, velocities, accelerations of a fixed point in the end-effector.

(ii) A sequence of orientations, angular velocities and angular accelerations of the end-effector. The fixed point in the end-effector will be referred to as the tool center point and is denoted by TCP. The orientation of the end-effector is best described by a coordinate frame attached to the end-effector, referred to as the tool frame and is denoted by TF.

1.4. Motion Of A Robot End-Effector [2,3]

A typical robot trajectory is shown in Figure 1. The location and orientation of the robot end-effector are completely described using the tool frame (TF) and the tool center point (TCP). The tool frame consists of three unit vectors; namely, the orientation vector $\underline{O}$, the approach vector $\underline{A}$ and the normal vector $\underline{N}$. The tool center point TCP is chosen to be the origin of the tool frame.

1.5. Representation of a robot trajectory using a ruled surface

Each of the three unit vectors of the tool frame generates a ruled surface while the three ruled surfaces share a common direcrix traced (trajectory) by the TCP. It is not necessary to use all three ruled surfaces to represent a robot trajectory; in fact, one ruled surface will suffice. As shown in Figure 2, the ruled surface generated by the normal vector $\underline{N}$ is chosen here to represent the trajectory. We may note, however, that the orientation of other vectors, $\underline{A}$ and $\underline{O}$, are not specified yet. Theoretically, this is because a robot end-effector motion, in general, has six degrees of freedom in space while a ruled surface provides only five independent parameters. Therefore, a robot trajectory may be completely described by adding one parameter to specify the orientation of the two vectors. The additional parameter referred to, in this study, as the spin angle and denoted as η. The spin angle is measured from the surface normal vector $\underline{S}_n$ of the ruled surface to the normal vector $\underline{N}$ as shown in Figure 2. The ruled surface and the spin angle which completely describes a robot trajectory, respectively, are

$$\underline{X}(s,v) = \underline{\alpha}(s) + vR(s), \quad \eta = \eta(s), \tag{1.1}$$

where $\underline{\alpha}$ is the directrix , v is a real-values parameter, and $\underline{R}$ is the ruling. We choose the normal vector $\underline{N}$, to be the ruling. Any one of the three vectors in tool frame could be chosen as the ruling and the spin angle describes the orientation of the other two vectors in cyclic order.

There are four frames of reference which are essential in the study of the motion of the end-effectors which are costruction as the following (Fig.3):

(i) The tool frame $(\underline{O}, \underline{A}, \underline{N})$.

(ii) The surface frame $(\underline{N}, \underline{S}_n, \underline{S}_b)$.

(iii) The generator trihedron $(\underline{r}, \underline{t}^*, \underline{t}_c)$.

(iv) The natural trihedron $(\underline{t}^*, \underline{n}^*, \underline{b}^*)$.

The differential properties of the motion of the tool frame and the TCP are studied based on the curvature theory of the ruled surface, using the relationships between the four frames of reference.

2. Reference Frames

Each vector of tool frame in end-effector defines its own timelike ruled surface while robot moves. The path of tool center point is directrix and $\underline{N}$ is the ruling. As $\underline{\alpha}(s)$ is a spacelike curve and $\underline{R}(s)$ is spacelike straight line, let us take the following timelike ruled surface

$$\underline{X}(s,v) = \underline{\alpha}(s) + v\underline{R}(s). \tag{2.1}$$

The normalized parameter s may be based on the directrix $\underline{\alpha}$ or on the ruling $\underline{R}$ as in the following.

$$s(\varphi) = \int_0^{\varphi} |\frac{d\underline{\alpha}(\varphi)}{d\varphi}| d\varphi, \tag{2.2}$$

$$s(\varphi) = \int_0^{\varphi} |\frac{d\underline{R}(\varphi)}{d\varphi}| d\varphi. \tag{2.3}$$

Through out this paper we use the normalized parameter as in (2.3).

2.1. Surface frame

To determined the orientation of tool frame relative to the timelike ruled surface, we define a surface frame at the TCP as shown in Figure 3. The surface frame is defined by three orthogonal unit vectors, the orientation vector $\underline{O}$, the surface normal vector $\underline{S}_n$, and binormal vector $\underline{S}_b$. The surface normal vector is determined by using the definition of the normal vector to the surface

$$\underline{S}_n = \frac{\underline{X}_v \wedge \underline{X}_s}{|\underline{X}_v \wedge \underline{X}_s|}. \tag{2.4}$$

The surface binormal vector is

$$\underline{S}_b = \underline{S}_n \wedge \underline{N}. \tag{2.5}$$

2.2. Frenet frame

The frenet frame is defined by three orthogonal unit vectors, namely; the tangent vector $\underline{t}$, the normal vector $\underline{n}$, and the binormal vector $\underline{b}$, where

$$\underline{t} = \underline{\alpha}', \ \ \underline{n} = \frac{\underline{t}'}{k}, \ \ \underline{b} = \underline{n} \wedge \underline{t}, \tag{2.6}$$

where $k = |\underline{t}'|$, is the curvature of the directrix α.

2.3. Generator trihedron

Generator trihedron moves along the striction curve. Generator trihedron is used to study the positional and angular variation of ruled surface. The generator trihedron is defined by three orthogonal unit vector, namely; the generator vector $\underline{r}$, the central normal vector $\underline{t}$ and the central tangent vector $\underline{k}$. Since the ruling is not necessarily, so a unit vector, the generator vector (spacelike) is defined as

$$\underline{r} = \frac{\underline{R}}{R}. \tag{2.7}$$

The central normal vector (spacelike) is defined as

$$\underline{t^*} = R'. \tag{2.8}$$

The central tangent vector(timelike) is defined as

$$\underline{t}_c = \underline{t^*} \wedge \underline{r}. \tag{2.9}$$

The striction curve of timelike ruled surface is

$$\underline{\beta}(s) = \underline{\alpha}(s) - \mu(s)\underline{R}(s), \tag{2.10}$$

where μ is a real valued parameter, the distance from the striction curve to the directrix along the ruling is μR, where $R = |\underline{R}|$, by using the definition of the striction curve we have

$$\mu = \prec \alpha', R' \succ, \tag{2.11}$$

Differentiating Equation (2.9), gives the first order positional variation of the striction point of the timelike ruled surface expressed in the generator trihedron,

$$\underline{\beta}' = \Gamma \underline{r} + \Delta \underline{t}_c, \tag{2.12}$$

where

$$\begin{aligned}\Gamma &= \tfrac{1}{R} \prec \underline{\alpha}', R \succ -\mu' R \\ \Delta &= \tfrac{1}{R}[\alpha', R, R']\end{aligned}, \tag{2.13}$$

From a study of motion of generator trihedron and the striction curve, we can obtain the differential motion of the end-effector in a simple and systematic manner. The first-order angular variation of the generator trihedron defined in the following matrix

$$\frac{d}{ds}\begin{pmatrix} \underline{r} \\ \underline{t}^* \\ \underline{t}_c \end{pmatrix} = \frac{1}{R}\begin{pmatrix} 0 & 1 & 0 \\ -1 & 0 & \gamma \\ 0 & -\gamma & 0 \end{pmatrix}\begin{pmatrix} \underline{r} \\ \underline{t}^* \\ \underline{t}_c \end{pmatrix} = U_r \wedge \begin{pmatrix} \underline{r} \\ \underline{t}^* \\ \underline{t}_c \end{pmatrix}, \tag{2.14}$$

where

$$\gamma = \prec R'', (R \wedge R') \succ, \tag{2.15}$$

$$U_r = \frac{-1}{R}\underline{t}_c + \frac{\gamma}{R}\underline{r}, \tag{2.16}$$

is the Darboux vector of the generator trihedron.

2.4. Darboux frame for the ruled surface X

The Darboux frame for a ruled surface X is defined by three orthogonal unit vector, namely; the tangent vector $\underline{T}$ the normal vector $\underline{S}_N$ and the geodesic vector $\underline{n}_g$.

$$\underline{T} = \frac{dx}{ds} = \underline{t} + v\underline{t}^* - \frac{v'}{R}(\mu - v \mid R \mid)\underline{r}, \tag{2.17}$$

$$\underline{S}_N = \frac{X_1 \wedge X_2}{\mid X_1 \wedge X_2 \mid} = \frac{v'}{\Pi}((\mu + v \mid R \mid)\underline{t}_c + \frac{v'}{R}\underline{t}^*), \tag{2.18}$$

where, $\Pi = \sqrt{(\mu - v \mid R \mid)^2 + \Delta^2}$

$$\underline{n}_g = \underline{T} \wedge \underline{S}_N = \frac{1}{\Pi}((\mu - v \mid R \mid)(\underline{t} \wedge \underline{t}_c)) - \Delta(\underline{t} \wedge \underline{t}^* + v(\mu - v \mid R \mid)\underline{r} + \frac{v'(\mu - v \mid R \mid)}{\mid R \mid}\underline{t}^* - \frac{v\Delta'}{\mid R \mid}\underline{t}_c), \tag{2.19}$$

2.5. Central normal surface and natural trihedron

The natural trihedron used to study the angular and positional variation of the central normal surface. As the generator trihedron moves along the striction curve, the central normal vector generates another ruled surface called the central normal surface. The central normal surface, is defined as

$$\underline{X}_T(s,v) = \underline{\beta}(s) + v\underline{t}^*(s), \tag{2.20}$$

where $\underline{\beta}$ is the position vector of the striction line of the original ruled surface, and v is areal parameter. The location of the striction curve of the central normal surface relative to the striction curve of the ruled surface is given by

$$\underline{\beta}_T(s) = \underline{\beta}(s) - \mu_T\, \underline{t}^*(s), \tag{2.21}$$

where,

$$\mu_T(s) = \left| \frac{\prec \beta', t^{*\prime} \succ}{\prec t^{*\prime}, t^{*\prime} \succ} \right|. \tag{2.22}$$

From equation (2.11) and (2.13), we have

$$\mu_T(s) = \frac{R(-\Gamma + \Delta\gamma)}{1-\gamma^2}. \tag{2.23}$$

The natural trihedron is defined by three orthogonal unit vector, namely; the central normal vector $\underline{t}^*$ (spacelike), the principal normal vector $\underline{n}^*$ (spacelike) and the binormal vector $\underline{b}^*$ (timelike) as following:

$$\underline{t}^* = \underline{R}', \tag{2.24}$$

$$\underline{n}^* = \frac{1}{\kappa^*}\underline{t}^{*\prime}, \tag{2.25}$$

$$\kappa^* = |\underline{t}^{*\prime}|, \tag{2.26}$$

$$\underline{b}^* = \underline{n}^* \wedge \underline{t}^*. \tag{2.27}$$

The frenet frame for the central normal surface is defined as the tangent vector $\underline{t}_T$, the normal vector $\underline{n}_T$, and the binormal vector $\underline{b}_T$, where .

$$\underline{t}_T = \underline{\beta}', \tag{2.28}$$

$$\underline{n}_T = \frac{\underline{t}_T{}'}{|\underline{t}_T{}'|}, \tag{2.29}$$

$$\underline{b}_T = \underline{n}_T \wedge \underline{t}_T. \tag{2.30}$$

Let ρ be the rotation angle between spacelike vector $\underline{r}$ and timelike vector $\underline{b^*}$, where

$$\begin{aligned} \underline{r^*} &= -i\cosh\rho\ \ \underline{b^*} + i\sinh\rho\ \ \underline{n^*} \\ \underline{t}_c &= \underline{t^*}\wedge\underline{r} = i\cosh\rho\ \ \underline{n^*} - i\sinh\rho\ \ \underline{b^*} \end{aligned}, \tag{2.31}$$

Equation (2.31) can be written in matrix form as

$$\begin{pmatrix} \underline{r} \\ \underline{t^*} \\ \underline{t}_c \end{pmatrix} = \begin{pmatrix} 0 & i\sinh\rho & -i\cosh\rho \\ 1 & 0 & 0 \\ 0 & i\cosh\rho & -i\sinh\rho \end{pmatrix} \begin{pmatrix} \underline{t^*} \\ \underline{n^*} \\ \underline{b^*} \end{pmatrix}, \tag{2.32}$$

by the inverse of the equation (2.32), then

$$\begin{pmatrix} \underline{t^*} \\ \underline{n^*} \\ \underline{b^*} \end{pmatrix} = \begin{pmatrix} 0 & 1 & 0 \\ i\sinh\rho & 0 & -i\cosh\rho \\ i\cosh\rho & 0 & -i\sinh\rho \end{pmatrix} \begin{pmatrix} \underline{r} \\ \underline{t^*} \\ \underline{t}_c \end{pmatrix}. \tag{2.33}$$

From equation (2.13),(2.21) and (2.26), we have

$$\underline{t^*}' = \frac{1}{R}(-\underline{r} + \gamma\underline{t}_c) = \kappa^*\underline{n^*} = \kappa^*(i\sinh\rho\ \underline{r} - i\cosh\rho\ \underline{t}_c), \tag{2.34}$$

then, we have

$$\sinh\rho = \tfrac{i}{R\kappa^*}, \qquad \cosh\rho = \tfrac{i\gamma}{R\kappa^*}\ , \tag{2.35}$$

Then the geodesic curvature may also be written as

$$\gamma = \coth\rho \tag{2.36}$$

substitute from equation (2.29) into equation (2.13), then

$$\frac{d}{ds}\begin{pmatrix} \underline{r} \\ \underline{t^*} \\ \underline{t}_c \end{pmatrix} = \frac{1}{R}\begin{pmatrix} 0 & 1 & 0 \\ -1 & 0 & \coth\rho \\ 0 & -\coth\rho & 0 \end{pmatrix} \begin{pmatrix} \underline{r} \\ \underline{t^*} \\ \underline{t}_c \end{pmatrix} = U_r \wedge \begin{pmatrix} \underline{r} \\ \underline{t^*} \\ \underline{t}_c \end{pmatrix}. \tag{2.37}$$

The Darboux vector of the generator trihedron is

$$U_r = \frac{-1}{R}\underline{t}_c + \frac{\coth\rho}{R}\ \underline{r}, \tag{2.38}$$

From equation (2.19), we have

$$\mu_T(s) = -R \quad be \quad \sinh^2\rho\ \ (-\Gamma + \Delta\coth\rho), \tag{2.39}$$

also by equation (2.25), the curvature is defined by

$$\kappa^* = \frac{\sqrt{1-\gamma^2}}{R} = \frac{i}{R \ \sinh\rho}. \tag{2.40}$$

The first-order angular variation of natural trihedron may be expressed in the matrix form as

$$\frac{d}{ds}\begin{pmatrix} \underline{t}^* \\ \underline{n}^* \\ \underline{b}^* \end{pmatrix} = \begin{pmatrix} 0 & \kappa^* & 0 \\ \kappa^* & 0 & \tau^* \\ 0 & -\tau^* & 0 \end{pmatrix}\begin{pmatrix} \underline{t}^* \\ \underline{n}^* \\ \underline{b}^* \end{pmatrix} = U_t \wedge \begin{pmatrix} \underline{t}^* \\ \underline{n}^* \\ \underline{b}^* \end{pmatrix}. \tag{2.41}$$

The Darboux vector of the natural trihedron is

$$U_t = \tau^* \underline{t}^*. \tag{2.42}$$

from equation (2.25) and (2.28), we have

$$\begin{pmatrix} \underline{r} \\ \underline{t}^* \\ \underline{t}_c \end{pmatrix} = \frac{1}{R\kappa}\begin{pmatrix} 0 & -1 & \gamma \\ R\kappa^* & 0 & 0 \\ 0 & -\gamma & 1 \end{pmatrix}\begin{pmatrix} \underline{t}^* \\ \underline{n}^* \\ \underline{b}^* \end{pmatrix}. \tag{2.43}$$

By the inverse of the equation (2.36), then

$$\begin{pmatrix} \underline{t}^* \\ \underline{n}^* \\ \underline{b}^* \end{pmatrix} = \frac{1}{R\kappa^*}\begin{pmatrix} 0 & R\kappa^* & 0 \\ -1 & 0 & \gamma \\ -\gamma & 0 & 1 \end{pmatrix}\begin{pmatrix} \underline{r} \\ \underline{t}^* \\ \underline{t}_c \end{pmatrix} \tag{2.44}$$

Substitute from Eq(2.36) into Eq(2.15), then we have

$$U_t = -\kappa^* \underline{b}^*. \tag{2.45}$$

Differentiating Equation (2.17) and from equation (2.36), (2.33) and (2.19), then the first order positional variation of the striction curve of central normal surface defined by

$$\underline{\beta}'_T = \Gamma_T \underline{t}^* + \Delta_T \underline{b} + \Pi_T \underline{n}^*, \tag{2.46}$$

where

$$\begin{aligned} \Gamma_T &= \mu'_T \ , \\ \Delta_T &= \frac{\gamma\Gamma - \Delta}{\sqrt{1-\gamma^2}} \ , \\ \Pi_T &= \frac{-2\Delta\gamma}{\sqrt{1-\gamma^2}} \ . \end{aligned} \tag{2.47}$$

Also we can find that

$$\kappa^{*2} = \frac{\prec (\underline{R}' \wedge \underline{R}''), (\underline{R}' \wedge \underline{R}'') \succ}{(\prec \underline{R}', \underline{R}' \succ)^3}, \tag{2.48}$$

$$\tau^{*} = \frac{[\underline{R}''', \underline{R}', \underline{R}'']}{\prec (\underline{R}' \wedge \underline{R}''), (\underline{R}' \wedge \underline{R}'') \succ}. \tag{2.49}$$

Observe that the Darboux vector of the generator trihedron, Eq(2.15) and the Darboux vector of the natural trihedron, Eq(2.35), describe the angular motion of the timelike ruled surface and the central normal surface, respectively. Therefor, the Darboux vector may be considered as the angular velocity, where as the positional variation of the striction curve may be considered as the linear velocity . We also note that the functions, Δ_T, Γ_T and Π_T in Eq.(2.39) and κ^* and τ^* in Eq.(2.40)and (2.41), play the same role as the curvature function of the central normal surface.

3. Relationship between the Frames of Reference

The orientation of the surface frame relative to the tool frame and the generator trihedron is shown in Figure 2. Let ϕ be the hyperbolic angle between the timelike vectors $\underline{S}_b$ and $\underline{A}$, then we have

$$\prec \underline{S}_b, \underline{A} \succ = \cosh\phi. \tag{3.1}$$

$$\underline{A} = \cosh\phi\ \underline{S}_b + \sinh\phi\ \underline{S}_n, \quad \underline{O} = \underline{A} \wedge \underline{N} = \cosh\phi\ \underline{S}_n + \sinh\phi\ \underline{S}_b. \tag{3.2}$$

These vectors can be written in matrix form as follows

$$\begin{pmatrix} \underline{N} \\ \underline{A} \\ \underline{O} \end{pmatrix} = \begin{pmatrix} 1 & 0 & 0 \\ 0 & \sinh\phi & \cosh\phi \\ 0 & \cosh\phi & \sinh\phi \end{pmatrix} \begin{pmatrix} \underline{N} \\ \underline{S}_n \\ \underline{S}_b \end{pmatrix}. \tag{3.3}$$

The inverse of this matrix is

$$\begin{pmatrix} \underline{N} \\ \underline{S}_n \\ \underline{S}_b \end{pmatrix} = \begin{pmatrix} 1 & 0 & 0 \\ 0 & -\sinh\phi & \cosh\phi \\ 0 & \cosh\phi & -\sinh\phi \end{pmatrix} \begin{pmatrix} \underline{N} \\ \underline{A} \\ \underline{O} \end{pmatrix}. \tag{3.4}$$

Let ψ be the hyperbolic angle between the timelike vectors $\underline{S}_b$ and $\underline{t}_c$ then, we have

$$\underline{t}_c = \cosh\psi\, \underline{S}_b + \sinh\psi\, \underline{S}_n \underline{t^*} = \underline{t}_c \wedge \underline{r} = \cosh\psi\, \underline{S}_n + \sinh\psi\, \underline{S}_b \tag{3.5}$$

or,

$$\begin{pmatrix} \underline{r} \\ \underline{t^*} \\ \underline{t}_c \end{pmatrix} = \begin{pmatrix} 1 & 0 & 0 \\ 0 & \cosh\psi & \sinh\psi \\ 0 & \sinh\psi & \cosh\psi \end{pmatrix} \begin{pmatrix} \underline{N} \\ \underline{S}_n \\ \underline{S}_b \end{pmatrix}. \tag{3.6}$$

The inverse of this matrix is

$$\begin{pmatrix} \underline{N} \\ \underline{S}_n \\ \underline{S}_b \end{pmatrix} = \begin{pmatrix} 1 & 0 & 0 \\ 0 & \cosh\psi & -\sinh\psi \\ 0 & -\sinh\psi & \cosh\psi \end{pmatrix} \begin{pmatrix} \underline{r} \\ \underline{t^*} \\ \underline{t}_c \end{pmatrix}. \tag{3.7}$$

From Eq.(3.5) and Eq.(3.2), then

$$\begin{pmatrix} \underline{N} \\ \underline{A} \\ \underline{O} \end{pmatrix} = \begin{pmatrix} 1 & 0 & 0 \\ 0 & \sinh\theta & \cosh\theta \\ 0 & \cosh\theta & \sinh\theta \end{pmatrix} \begin{pmatrix} \underline{r} \\ \underline{t^*} \\ \underline{t}_c \end{pmatrix}, \tag{3.8}$$

where $\theta = \phi - \psi$, the inverse of this matrix is

$$\begin{pmatrix} \underline{r} \\ \underline{t^*} \\ \underline{t}_c \end{pmatrix} = \begin{pmatrix} 1 & 0 & 0 \\ 0 & -\sinh\theta & \cosh\theta \\ 0 & \cosh\theta & -\sinh\theta \end{pmatrix} \begin{pmatrix} \underline{N} \\ \underline{A} \\ \underline{O} \end{pmatrix}, \tag{3.9}$$

where, θ referred to spin angle that describes the orientation of the end-effector. Substituting the partial derivatives of Equation (2.1) into (2.4) then we have

$$\underline{S}_n = \frac{\mu \underline{k} + \Delta \underline{t}}{\sqrt{\Delta^2 - \mu^2}}, \tag{3.10}$$

and

$$\underline{S}_b = \underline{N} \wedge \underline{S}_n = \frac{\mu \underline{t^*} + \Delta \underline{t}_c}{\sqrt{\Delta^2 - \mu^2}}. \tag{3.11}$$

From equation (3.6), (3.9), (3.10) we have

$$\cosh\psi = \frac{\Delta}{\sqrt{\Delta^2 - \mu^2}}, \qquad \sinh\psi = \frac{-\mu}{\sqrt{\Delta^2 - \mu^2}} . \tag{3.12}$$

4. Differential properties of the robot end effector motion

The motion of the robot end effector is described by the angular motion of the tool frame and the linear motion of the TCP. In this section, the differential motion properties of the tool frame and TCP are studied

4.1. First order properties

Since the directrix $\underline{\alpha}$ is the locus of the TCP, by taking the derivative of equation (2.9), we have

$$\underline{\alpha}'(s) = \underline{\beta}' + \mu'\underline{R} + \mu\underline{t}^*. \tag{4.1}$$

From Eq.(2.11), we have

$$\underline{\alpha}'(s) = (\Gamma + \mu' R)\underline{r} + \mu\underline{t}^* + \Delta\underline{t}_c. \tag{4.2}$$

From Eq.(3.7), we have

$$\underline{\alpha}'(s) = (\Gamma + \mu' R)\underline{N} + (\Delta\cosh\theta - \mu\sinh\theta)\underline{A} + (\mu\cosh\theta - \Delta\sinh\theta)\underline{O}. \tag{4.3}$$

To determined the first order angular variation of the tool frame, we taking the derivative Eq,(3.6), we have

$$\frac{d}{ds}\begin{pmatrix}\underline{N}\\ \underline{A}\\ \underline{O}\end{pmatrix} = \frac{1}{R}\begin{pmatrix} 0 & 1 & 0\\ -\sinh\theta & (\Omega-\gamma)\cosh\theta & (\Omega+\gamma)\sinh\theta\\ -\cosh\theta & (\Omega-\gamma)\sinh\theta & (\Omega+\gamma)\cosh\theta \end{pmatrix}\begin{pmatrix}\underline{r}\\ \underline{t}^*\\ \underline{t}_c\end{pmatrix}. \tag{4.4}$$

where $\Omega = \theta' R$, substitute from Eq.(3.7) into Eq.(4.4) then, we have

$$\frac{d}{ds}\begin{pmatrix}\underline{N}\\ \underline{A}\\ \underline{O}\end{pmatrix} = \frac{1}{R}\begin{pmatrix} 0 & -\sinh\theta & \cosh\theta\\ -\sinh\theta & \gamma\sinh 2\theta & \Omega-\gamma\cosh 2\theta\\ -\cosh\theta & \Omega+\cosh 2\theta & -\gamma\sinh 2\theta \end{pmatrix}\begin{pmatrix}\underline{N}\\ \underline{A}\\ \underline{O}\end{pmatrix}. \tag{4.5}$$

Eq.(4.5) can be writhen as

$$\frac{d}{ds}\begin{pmatrix}\underline{N}\\ \underline{A}\\ \underline{O}\end{pmatrix} = \underline{U}_o \wedge \begin{pmatrix}\underline{N}\\ \underline{A}\\ \underline{O}\end{pmatrix}, \tag{4.6}$$

where

$$\underline{U}_o = \frac{-1}{R}\cosh 2\theta\, \underline{N}, \tag{4.7}$$

is referred to as the Darboux vector of the tool frame, from Eq.(3.6) we have

$$\underline{U}_o = \frac{-1}{R}\cosh 2\theta \; \underline{r}, \tag{4.8}$$

also from Eq(2.15), we have

$$\underline{U}_o = \cosh 2\theta[\frac{1}{R\gamma}\underline{t}_c - \frac{1}{\gamma}U_r]. \tag{4.9}$$

4.2. Second order properties

Differentiating Eq.(4.2), we have

$$\underline{\alpha}''(s) = (\Gamma' + \mu'' R - \frac{\mu}{R})\underline{r} + (\frac{\Gamma}{R} + 2\mu' + \frac{\Delta\gamma}{R})\underline{t^*} + (\Delta' + \frac{\mu\gamma}{R})\underline{t}_c. \tag{4.10}$$

This can be expressed by the tool frame, from Eq.(3.7), we have

$$\begin{aligned}\underline{\alpha}''(s) = (\Gamma' + \mu'' R - \tfrac{\mu}{R})\underline{N} + [(\Delta' + \tfrac{\mu\gamma}{R})\cosh\theta - (\tfrac{\Gamma}{R} + 2\mu' - \tfrac{\Delta\gamma}{R})\sinh\theta]\underline{A} + \\ [(\tfrac{\Gamma}{R} + 2\mu' - \tfrac{\Delta\gamma}{R})\cosh\theta - (\Delta' + \tfrac{\mu\gamma}{R})\sinh\theta]\underline{O}\end{aligned} \tag{4.11}$$

Take the derivative of Eq.(4.8)

$$\underline{U}_o' = \frac{1}{R^2}(-2R\sinh 2\theta \underline{r} - \cosh 2\theta)\underline{t^*}. \tag{4.12}$$

Also by differentiating Eq(2.38) and (2.45), we have

$$\underline{U}_r' = \kappa^*\tau^*\underline{n^*} - \kappa^{*\prime}\underline{b^*}, \tag{4.12}$$

$$\underline{U}_t' = \tau^{*\prime}\underline{t^*} + \tau^*\kappa^*\underline{n^*}. \tag{4.13}$$

By continuing the differentiation, we also can obtain higher order properties of the end effector motion. However, we may use only up to second order properties of motion in current robot control technology.

4.3. Linear and angular velocity and acceleration of a robot end effector

Since the robot trajectory planning is based on time-dependent properties, eg., velocity, acceleration, angular velocity, and angular acceleration, of robot end effector motion. The time-dependent motion properties of the end effector can be determined by applying the chain role to the differential motion properties that determined in section (4.2).

The velocity and acceleration of TCP, angular velocity, and acceleration of the end effector are determined, respectively as

$$\begin{aligned} &\underline{V} = \underline{\alpha}'\dot{s}, \qquad \underline{a} = \underline{\alpha}'\ddot{s} + \underline{\alpha}''\dot{s}^2, \\ &\underline{w} = \underline{U}_o\dot{s}, \qquad \underline{\vartheta} = \underline{\dot{w}} = \underline{U}_o\ddot{s} + \underline{U}_o'\dot{s}^2, \end{aligned} \tag{4.14}$$

where $. = \frac{d}{dt}$ (differentiation with respect to time).

5. Example

For a ruled surface

$$\underline{X}(s,v) = (\sqrt{2}\sin s, -\sqrt{2}\cos s, -s) + v(\cos s, \sin s, \frac{\sqrt{2}}{2}) \tag{5.1}$$

The striction curve is $\underline{\alpha}(s) = (\sqrt{2}\sin s, -\sqrt{2}\cos s, -s)$ where $\prec \underline{\alpha}', \underline{\alpha}' \succ = 1 > 0$ so $\underline{\alpha}(s)$ is spacelike vector and the generator is $\underline{R}(s) = (\cos s, \sin s, \frac{\sqrt{2}}{2})$ where $\prec \underline{R}, \underline{R} \succ = \frac{1}{\sqrt{2}} > 0$ so $\underline{R}(s)$ is spacelike vector

The vectors of generator trihedron are the following

$$\begin{aligned} &\underline{r} = \tfrac{\underline{R}}{R} = (\sqrt{2}\cos s, \sqrt{2}\sin s, 1) \qquad (spacelike\ vector) \\ &\underline{t^*} = \underline{R}' = (-\sin s, \cos s, 0) \qquad (spacelike\ vector) \\ &\underline{t}_c = (-\cos s, -\sin s, \sqrt{2}) \qquad (timelike\ vector) \end{aligned} \tag{5.2}$$

from Eq(2.10), (2.12), (2.14), (2.40) and (2.41), we have

$$\begin{aligned} &\Gamma = 1, \Delta = -2\sqrt{2}, \\ &\gamma = \tfrac{1}{\sqrt{2}}, \mu = 0, \\ &\kappa^* = 1. \end{aligned} \tag{5.3}$$

The three vectors of the natural trihedron are

$$\begin{aligned} &\underline{t^*} = (-\sin s, \cos s, 0) \qquad (spacelike\ vector) \\ &\underline{n^*} = (-\cos s, -\sin s, 0) \qquad (spacelike\ vector) \\ &\underline{b^*} = (0,0,1) \qquad (timelike\ vector) \end{aligned} \tag{5.4}$$

The Darboux vector of the generator trihedron is

$$\underline{U}_r = (2\sqrt{2}\cos s, 2\sqrt{2}\sin s, 2). \tag{5.6}$$

The Darboux vector of the natural trihedron is

$$\underline{U}_t = (0,0,1). \tag{5.7}$$

From Eq.(2.59), we have

$$\cosh\psi = \frac{-2\sqrt{2}}{\sqrt{8-\mu^2}}, \qquad \sinh\psi = \frac{-\mu}{\sqrt{8-\mu^2}}. \tag{5.8}$$

Then we have

$$\tanh\psi = \frac{2\sqrt{2}}{\mu}. \tag{5.9}$$

So the first derivative of ψ is

$$\psi' = \frac{2\sqrt{2}\mu'}{\mu^2-8}. \tag{5.10}$$

Since the spin angle between the tool frame and the surface is zero $\psi = 0 \to \psi' = 0$, then $\theta = \phi, \theta' = \phi'$. Then

$$\Omega = \frac{1}{\sqrt{2}}\psi'. \tag{5.11}$$

The approach vector and the normal vector are

$$\underline{A} = \frac{1}{\sqrt{8-\mu^2}}(32\sqrt{2}\sin s + 2\sqrt{2}\mu\cos s, 32\sqrt{2}\cos s + 2\sqrt{2}\mu\sin s, -4\mu). \tag{5.12}$$

$$\underline{O} = \frac{1}{\sqrt{8-\mu^2}}(-2\sqrt{2}\mu\sin s - 32\sqrt{2}\cos s, -2\sqrt{2}\mu\cos s - 32\sqrt{2}\sin s, 64). \tag{5.13}$$

The first and second order positional variation of the TCP can expressed in the tool frame as

$$\underline{\alpha}' = (1-2\mu')\underline{N} + \frac{32}{\sqrt{8-\mu^2}}\underline{A} + \frac{-8-\mu^2}{\sqrt{8-\mu^2}}\underline{O}, \tag{5.14}$$

and

$$\underline{\alpha}'' = (2\mu'' - \frac{\mu}{2})\underline{N} + \frac{-8}{\sqrt{8-\mu^2}}(\mu^2+2\mu'+197)\underline{A} + \frac{-\mu}{\sqrt{8-\mu^2}}(2\mu^2+315)\underline{O}. \tag{5.15}$$

The Darboux vector of the tool frame is

$$\underline{U}_o = \frac{-8-\mu^2}{8-\mu^2}\underline{N}. \tag{5.16}$$

The first order derivative of the Darboux vector of the tool frame is

$$\underline{U}_o' = \frac{1}{4\sqrt{8-\mu^2}}(4\underline{r} - (8+\mu^2)\underline{t}^*. \tag{5.17}$$

Conclusions

From the previous investigation, one can see that the motion of the robot end-effector can be represented by the union of ruled surface X and its associated central normal surface X_T. The configuration space consists of $X \cup X_T$ and the different frames with the orientation of the motion through the darboux frames, especially, U_0. The configuration space is given in Figure 1,2,3. The analytical representation is given through the frames attached to the ruled surfaces X and X_T which as described by the vector valued vectors $\underline{r}, \underline{t^*}, \underline{t_c}, \underline{n^*}, \underline{b^*}, \underline{U_r}, \underline{U_t}, \underline{U_0}; \underline{A}, \underline{O}, \underline{N}$ and the spin angle.

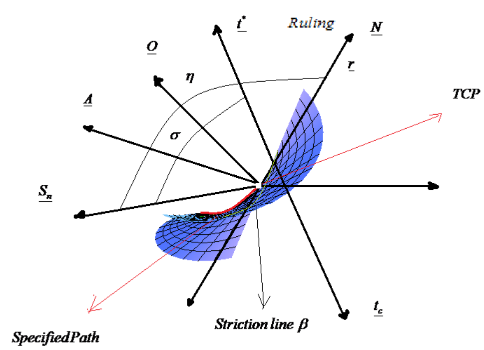

FIGURE 1. A ruled surface and frams of reference

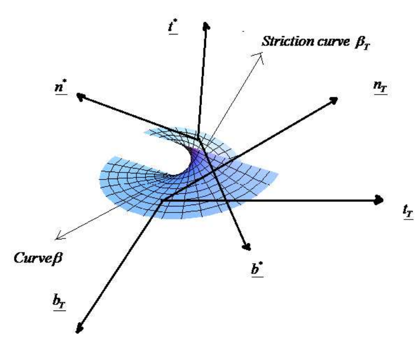

FIGURE 2. The central normal surface and frams of reference

Conflict of Interests

The authors declare that there is no conflict of interests.

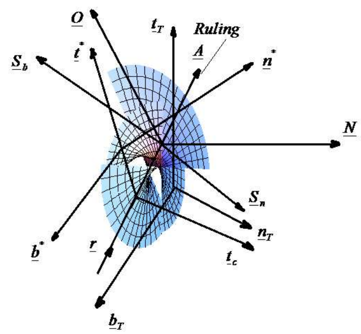

FIGURE 3. The configuration space of the motion $X \cup X_T$

Acknowledgement

The authors would like to thank Prof. Dr. Nassar Hassan Abdel-All, Emeritus Professor, Department of Mathematics, Faculty of Science, Assiut University for helpful discussions and valuable suggestions about the topic of this paper.

REFERENCES

[1] Rawya A. Hussein, Ali Abdela Ali, Geometric visualization of a Robot End-effector motion using The Curvature Theory Part-I, Mitteilungen Klosterneuburg, 65 (2015), 191-210.

[2] Nassar H. Abdel-All, Rawya A. Hussein, Ali Abdela Ali, Bress Complex Ruled Surface Of A Rigid Body Motion Using Dual Calculus, Ciencia e tecnica, 30 (2015), 124-140.

[3] Nassar H. Abdel-All et al; Ruled surfaces with timelike rullings. Applied Math. and computations, 147 (2004), 241-253.

[4] B. S. Ryuh, G. R. Pennock; Accurate motion of Robot End-Effector using the curvature theory of ruled surfaces, J. Of Mechanisms, Transmissions, and Automation in Design, 110 (1988), 383-387.

[5] C. Ekici, Yasin Unl*ü*t*ü*rk, Mustafa Dede and B. S. Ryuh; On Motion of Robot End-effector Using The Curvature Theory of Timelike Ruled Surfaces With Timelike Ruling, Mathematical Problems in Engineering, 2008 (2008), Article ID 362783.

[6] Vladimir M. Zatsiorsky; Kinematics of Human motion, Library of Congress (1998).

[7] Helmut Pottmann and Johannes Wallner; Computational Line geometry, Springer-Verlag Berlin (2001).

[8] B. Chow and D. Tsai, Nonhomogeneous Gauss curvature flows, Indiana Univ. Math. J. 47 (1998), 965-994.